DE-EE0005963

High Efficiency, Low EMI and Positioning Tolerant Wireless Charging of EVs

Submitted by:
Principal Investigator:
Rakan Chabaan, Senior Engineer
Hyundai America Technical Center Inc.
E: rchabaan@hatci.com
P: 734-337-2305

Prepared for:
United States Department of Energy
National Energy Technology Laboratory

December 2017

NATIONAL ENERGY TECHNOLOGY LABORATORY

HYUNDAI MOTOR GROUP

MOJO MOBILITY

Acknowledgements

This material is based on work supported by the U.S. Department of Energy under Award DE-EE0005963.

We also would like to thank Mojo Mobility and its CEO Afshin Partovi. Additional Mojo Mobility contributors included senior software engineer Ken Ho, senior electrical engineer Michael Eliashberg, and hardware systems engineer Pouyan Shams. From the Idaho National Laboratory Electric Vehicle Infrastructure laboratory, we thank principal researcher Richard “Barney” Carlson, and advanced vehicle research engineer Shawn Salisbury. Appreciation also goes to United Laboratories and Navigant Research. At HATCI, personal thanks to test engineer Bilal Javaid and project budget manager John Robb.

Disclaimer

Abstract

The objective of this project is to develop, implement, and demonstrate a wireless power transfer (WPT) system that is capable of the following metrics:

- Total system efficiencies of more than 85 percent with minimum 20 cm coil-to-coil gap.
- System output power at least 6.6 kW; but design system up to 19.2 kW for future higher power study.
- Maximum lateral positioning tolerance achievable while meeting regulatory emission guidelines.

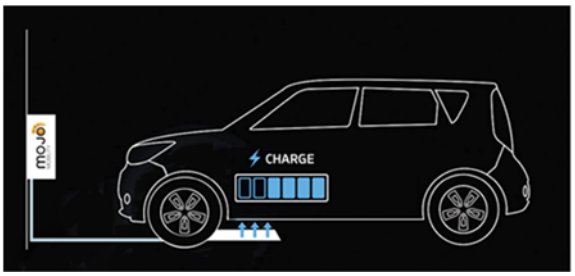

Figure 1: Wireless charging transfer system with receiver.

Table of Contents

Executive Summary

In 2012, Hyundai-Kia America Technical Center, Inc. (HATCI), and Mojo Mobility Inc. (Mojo), partnered to develop a wireless power transfer (WPT) system for plug-in electric vehicles (PEVs). The system was developed, implemented and demonstrated over the course of five years using five Kia Soul electric vehicles (EVs).

HATCI, the North American technology and engineering division of Korean-based automaker Hyundai Motor Group (HMG), and Mojo Mobility, a leader in mobile wireless charging technologies, used Mojo's patented Near Field Power® (NFP®) technology, to create an advanced WPT prototype to overcome several limitations of current wireless charging technology.

Mojo's proprietary technology localized the magnetic field and provided a low reluctance path for the return of the magnetic field. This allowed significantly higher power transfer efficiencies, lower electromagnetic field (EMF) emissions into the environment, larger coil-to-coil lateral misalignment and greater vertical gap separation between the ground transmitter (Tx) and the receiver (Rx).

The program goals included developing, implementing and demonstrating a WPT system with:

- Power transfer exceeding 6.6 kW
- Total system efficiency of at least 85 percent
- A vertical gap between the ground transmitter and receiver of 20 cm
- Integration into five Kia Soul EVs allowing wireless charging

The overall program was developed, implemented and demonstrated in three phases. During Phase I, the WPT system was created in a laboratory environment using a 240-volt single phase input maximizing coil-to-coil lateral alignment. Mojo was responsible for the Phase I technology development and assisted with the technology integration into the first Kia Soul EV development vehicle during Phase II. During Phase III, extensive testing was conducted at HATCI and independently at the Idaho National Laboratory (INL). The WPT was integrated into five Kia Soul EVs and real-world demonstrations were conducted. One of the vehicles was provided to the Department of Energy's Idaho National Laboratory for testing.

Accomplishments

HATCI and Mojo successfully validated that the WPT system was able to achieve a 10 kW power transfer, significantly higher than the DOE requirement. With further development and testing, it is possible to achieve wireless charging at power levels higher than 10 kW. The HATCI WPT system was designed for power transfer of up to 19.2 kW.

The 20 cm coil-to-coil vertical z-gap separation was verified as providing practical, safe and efficient power transmission during static testing. In part because of a higher power transfer than many plug-in Level 1 and Level 2 conductive chargers, HATCI's WPT electronics system achieved a state- of- charge (SoC) from 5 percent to 94 percent in 210-220 minutes, 30-40 minutes faster than a wall-mounted plug-in conductive charging unit operating at 7 kW.

Several prototype and firmware updates of the WPT system contributing to a better understanding of the required constraints, component and material selection, system geometry and functional architecture. Integrating the WPT system into the Kia Soul EVs resulted in a more comprehensive grasp of automotive engineering in electromagnetic compatibility (EMC), charging system interoperability, wireless communication, electric vehicle impact safety, and system alignment.

One of the ongoing challenges for wireless power transfer is defining the effects of electromagnetic field (EMF) radiation exposure on people. The project included multiple measurements of EMF radiation using the 2010 public exposure limits established by the International Commission on Non-Ionizing Radiation Protection (ICNIRP). [(2011). Guidelines for Limiting Exposure to Time-Varying Electric and Magnetic Fields (1Hz to 100 KHz): Erratum. *Health Physics, 100* (1), 9.]

During testing, EMF radiation under and around the wireless charging vehicle at heights +/-20 cm above the ground were less than 10 percent of the 2010 ICNIRP guidelines. Electromagnetic field radiation emissions were less than 1 percent of ICNIRP public exposure limits inside the vehicle because of shielding provided by the metal engine wall on the stock EV. With two EVs parked side to side and head to head, EMF radiation was below the ICNIRP standard for all test conditions, except when the EMF measurement probe was exposed directly to the magnetic field under the vehicles.

When foreign objects were detected in the magnetic field between the transmitter and receiver, some high temperatures were reported, prompting the WPT system to shut off. [(2017) Laboratory Performance and Safety Test Results of the Hyundai/Mojo Mobility 7.0 kW WPT System, Richard Barney Carlson, Idaho National Laboratory, US]

Commercial Viability and Potential Public Benefits

According to a 2015 Navigant Research commercial viability analysis commissioned by HATCI, wireless charging is a pre-commercial market that would grow from about 300 systems in 2014 to 62,000 by 2024 mainly for premium vehicle buyers. [Jerram, L., Gartner, J., & Abuelsamid, S. (2015). *Wireless Charging Commercial Viability Analysis* (pp. 5-9, Publication). Navigant Research.]

At the time of the study, HATCI's wireless system, equipment, according to Navigant, cost about seven times the price of a conductive charger available through conventional channels. Navigant said its research showed wireless systems would initially need to be accompanied by conductive charging systems because of the relative scarcity of wireless charging. [Jerram, L., Gartner, J., & Abuelsamid, S. (2015). *Wireless Charging Commercial Viability Analysis* (p. 7, Publication). Navigant Research.]

According to a September 2017 report from marketsandmarkets.com, the wireless EV charging market is projected to grow at a compound annual growth rate of 49.38 percent from 2020 to 2025, to reach a market size of about $7.1 billion by 2025. The key factors driving the market for wireless EV charging are increasing demand for electric vehicles, increasing infrastructure for fast chargers and rising consumer demand for convenience features.

The public charging station is estimated to be the fastest growing application segment of the wireless EV charging market. As the sale of electric vehicles increase, there will be a corresponding need for more publicly accessible charging stations.

HATCI is evaluating its WPT system for commercial applications. If it moves to full production, the public would have an alternative to Level 2 conductive charging and Level 3 direct current (DC) fast charging. Drivers of gasoline-powered vehicles are accustom to parking their vehicles and walking away. With wireless charging, owners of plug-in hybrid (PHEVs) and battery electric vehicles (BEVs) would be able to enjoy the same convenience.

Project Objectives

In a typical Magnetic Resonant (MR) system developed for electric charging, as much as 80 percent of the magnetic field generated between the transmitting and receiving coils can be leaked to surroundings at a coil-to-coil offset of 20 cm and laterally offset coils. The large amount of radiation resulting in large electromagnetic interference with the adjacent electrical and electronics systems, health concerns from EMF radiation and the low efficiency in the system is the most significant challenge facing wireless power charging of EVs.

HATCI and Mojo addressed these issues in a three-phase project to develop, implement and demonstrate a total wireless power transfer (WPT) system. During Phase I, the objective was to build a WPT system on a bench in a laboratory environment and to demonstrate wireless power system transfer at a minimum of 6.6 kW with at least 85 percent efficiency and a 20 cm vertical z-gap between the transfer and receiving coils at a frequency of 80 to 100 kHz. During Phase II, the WPT system was to integrate a WPT system into a Grid Connected Electric Vehicle (GCEV) and demonstrate the same power and transfer requirements as Phase I. During Phase III, the goals were to integrate the WPT system into four additional Kia Soul EVs, providing one of vehicles to the DOE's Idaho National Laboratory (INL) for independent testing and conducting WPT performance and safety testing on the other vehicles at HATCI.

Technical Challenges

At the time the HATCI project began, wireless charging for EVs typically used circular transmitter and receiver coils operating in resonance to transfer power between them. These WPT systems included magnetic field shielding behind the charger and/or receiver coils to guard the vehicle and surrounding areas from electronic interference and unwanted EMF radiation generated by the transmitter (charger).

The challenges included positioning the vehicle in proximity to the charger and methods for alerting and guiding the driver to successfully connect. This made a large alignment tolerance highly desirable.

Yet automobile design differences complicate receiver coil placement because manufacturers differ on the receiver coil's precise location. If transmitter coils are statically embedded, such as in a parking garage, the placement of the receiver and charger coil alignment cannot be guaranteed for all EVs.

A better magnetic coupling system including a low reluctance path for the return of the magnetic flux lines between the charger and receiver as in the Mojo design is necessary to reduce power loss, heating, and EMF radiation affecting nearby devices, vehicles and passengers. In several EV trials of Magnetic Resonant wireless charging by U.S. automobile manufacturers, high amounts of interference with automotive electronics systems were observed, causing malfunction and lockout of ignition and door lock systems. As mentioned above, Magnetic Resonant systems can suffer from large EMF emission problems.

Technical Approach

The HATCI/Mojo Mobility proposal attempted a novel technical approach to comprehensively address these issues.

The return paths of the AC magnetic flux behind the charger and receiver coils were designed and guided to provide a low-reluctance path by appropriately designing magnetic layers below the charger coil and above the receiver coil. Magnetic layers were extended beyond the charger and receiver coil areas to allow for the returning flux lines to close on themselves, resulting in lower power loss, higher efficiency and lower EMF emissions. Modeling and testing on lower power systems by Mojo Mobility showed that proper design of such a system could result in significantly higher system efficiency.

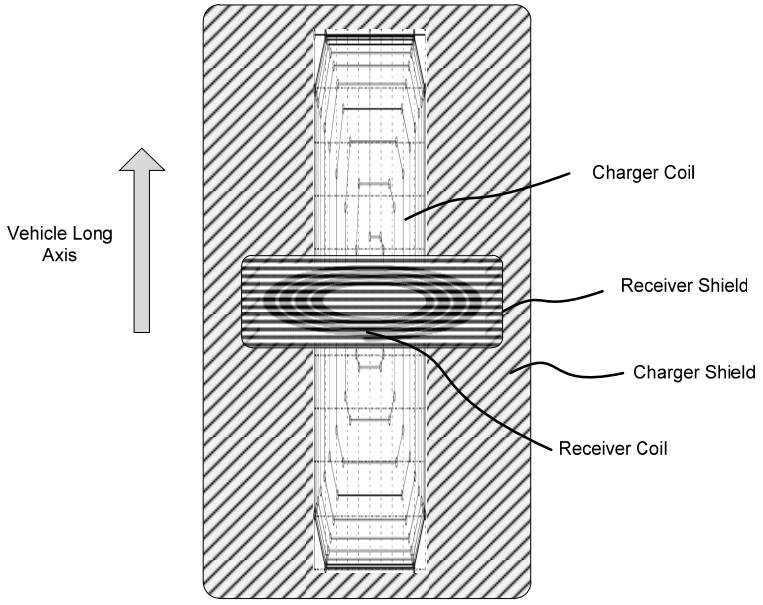

Figure 2: Design allowing wide range of positioning tolerance.

By using a crossed charger and receiver coil and shield geometry, overlap of some portion of the charger and receiver coil over a wide range along width of the vehicle (X) and along the length of the vehicle (Y) could be assured. This allowed large positioning tolerance in the design. The dimensions of the coils could be adjusted according to the positioning tolerance requirements and provide a highly flexible design platform. This design also provided a low-reluctance return path resulting in high efficiency and low EMF emissions.

Containing EMF emissions from the charger only to where the receiver is attached to the bottom of the vehicle is a key factor because excessive charger emissions would be emitted from other locations of the charger coil into the vehicle and surrounding areas. This would reduce system efficiency.

During Phase I, HATCI and Mojo modeled and fabricated a number of coils and associated magnetics to evaluate the effect of different designs. This included the X and Y positioning misalignment, and the coil z-gap on EMF radiation and maximum power transfer and efficiency.

Any practical WPT system development and implementation requires consideration of how susceptible the system is to nearby metallic parts. In a conventional magnetic resonant system, any metal sheet or part placed in between or near the coils during power transfer will absorb EMF radiation during power transfer causing high levels of dangerous heating due to localized currents setup by a pulsing magnetic field in a metal. This is the same operating principle as an inductive cooker, especially at frequencies greater than 100 kHz.

Project Activities:

An end-to-end block diagram and control interfaces were defined to establish a general understanding of energy and information exchange. An electrical simulation of the power chain from AC input to DC supply of an EV battery was produced. The team calculated the power efficiency estimates of the system based on simulations using real-world measurements of the key parameters of the coils developed.

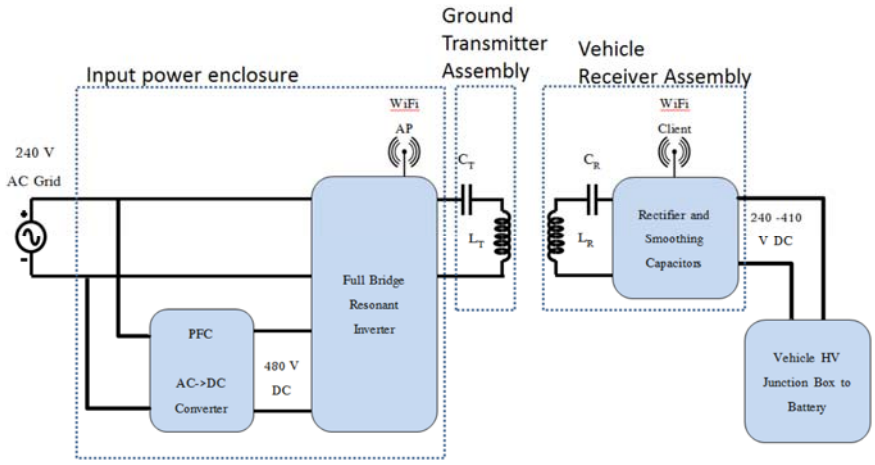

Figure 3: HATCI/Mojo Mobility WPT system electrical schematic overview.

The three major partitions of the WPT are the base station grid-connected power converter, which also includes a Power Factor Correction (PFC), AC to DC power converter, a transmitting coil (Tx) and the Receiver Coil and electronics (Rx). The Tx coil rests on the ground in a wireless charging parking space. It receives power from a high-frequency feed line coming from the power converter assembly and radiates a magnetic field for power coupling.

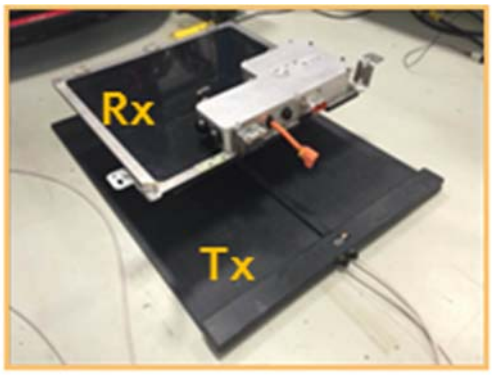

Figure 4: Wireless Power Transfer system with receiver (Rx) and transmitter (Tx)

The vehicle-mounted receiver (Rx) contains filtering components and wireless communications to initiate power transfer and feedback of control messages from the vehicle battery management system (BMS) and message sets for battery state-of-charge (SoC), charge rate and other necessary information. The Rx and the power converter communicate through Wi-Fi for power regulation and charging message communication.

Mojo Mobility's patented Near Field Power® (NFP®) technology localized the magnetic field and provided a low-reluctance return path for the magnetic field. This allowed significantly higher power transfer efficiencies, lower EMF emissions into the environment and larger coil-to-coil lateral misalignment and vertical gap separation. The result was practical, safe and efficient power transmission during static testing.

In Phase I, HACTI and Mojo developed the wireless power transfer system (WPT) with a minimum power transfer greater than 6.6 kW and a target of 19.2 kW. In addition, HATCI successfully maximized wireless power transfer coil-to-coil lateral misalignment while meeting regulatory guidelines. The target misalignment tolerance was +/-30 cm along the width of the vehicle and +/-40 cm along the length of the vehicle at a coil-to-coil z-gap of 20 cm.

In Phase II, the system was further developed and safely integrated into a Kia Soul EV. A commercial viability analysis of the system and cost benefits for components both on-board and off-board the vehicle was performed under a HATCI contract with Navigant Research. [Jerram, L., Gartner, J., & Abuelsamid, S. (2015). *Wireless Charging Commercial Viability Analysis* (pp. 5-9, Publication). Navigant Research.]

In Phase III, four additional Kia Soul EVs were equipped with the WPT system. One vehicle was tested independently at the Idaho National Laboratory (INL) and the others at HATCI. All required safety and electromagnetic field (EMF) emission and electromagnetic compatibility (EMC) test results and real-world performance results were provided to the DOE.

Phase I: Technology Development

The HATCI/Mojo team began developing the first generation of the High Efficiency, Low EMI and Positioning Tolerant Wireless Charging system in the first quarter of 2013. The focus was on the modeling and simulation of the WPT, particularly the electrical and electromagnetic modeling of the power transfer system based on further definition of the input power requirements and the energy system of the surrogate vehicle, a 2015 Kia Soul EV.

Figure 5: The 2015 Kia Soul EV was used as a surrogate vehicle with SAE J1772 standard compliance AC Level 1 and Level 2 charging as well as DC fast-charging CHArge de MOve" (CHAdeMO) infrastructure.

The main objective was to define the overall WPT system, including the component interfaces, projected future vehicle communications equipment, alignment strategy and voluntary standards development. To monitor this, the HATCI/Mojo team joined four SAE International task forces working on wireless charging standards.

The Phase I tasks included developing and updating System Requirement Specifications (SRS), reviewing target EV mechanical and electrical requirements, preliminary electrical, coil and magnetic modeling, and draft hardware and firmware system requirements. Once determined, coil and magnetic fabrication and firmware development for communications were integrated and tested.

The Phase I go/no-go criteria requirements were:

- At least 85 percent system efficiency after converting wall power 240-volt AC source to 480-volt high voltage DC.
- Greater than 6.6 kW power transfer in static charging.
- Minimum vertical gap spacing of 20 cm with data that showed maximum coil-to-coil misalignment in X and Y directions could meet EMF requirements.

HATCI and Mojo demonstrated it was possible to achieve total system efficiencies of more than 90 percent, power transfer at 10kW, and coil-to-coil positioning tolerance of +/-30 cm along the width of the vehicle and +/-40 cm along the length of the vehicle. Both were achieved at greater than 20 cm vertical coil-to-coil z-gap while meeting EMF guidelines.

Preliminary electromagnetic models of the transmitter and receiver coils were created to aid in fabrication specifications. The team simulated the electromagnetic fields between the transmitter (Tx) and receiver (Rx) coils to optimize the wireless power transfer capabilities of the physical system before full operational testing.

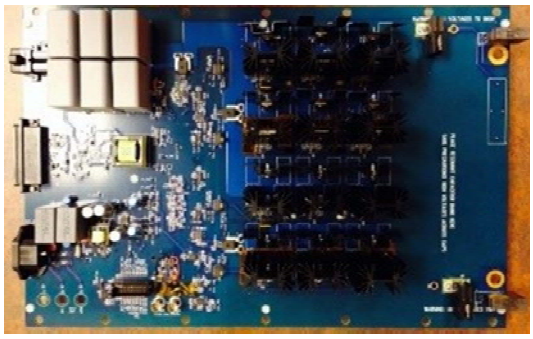

Figure 6: Gen 1 Transmitter (Tx).

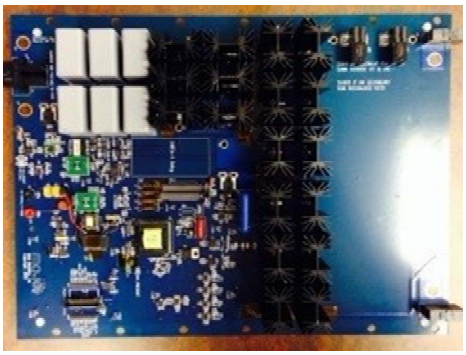

Figure 7: Gen 1 Receiver (Rx).

HATCI installed multiple 240V feeds at its Technical Center in Superior Township, Michigan, to provide a power input to the wireless charging system. An AC/DC power supply from an outside company was architected to support the requirements. Additional circuit simulations were conducted to help finalize voltage requirements for the front-end 240V.

The team designed, fabricated and tested standalone electrical hardware printed circuit boards (PCBs) for the transmitter and the receiver, verifying accurate simulation models of the electrical system with a focus on meeting all aspects of Phase I go/no-go requirements.

This was followed by testing Tx and Rx electrical hardware in the actual system setup. Power was applied to the system in a controlled, systematic method and wireless power transfer was demonstrated at lower power. Efficiency measurements were performed over different heights in the z-gap to compare performance differences to simulations. Electrical components and the PCBs were constantly monitored for performance deviations, temperature and electrical signal quality.

The Tx and Rx circuit boards successfully transferred power at levels representative of a vehicle battery and at a 21 cm coil-to-coil z-gap gap using a symmetric coil configuration.

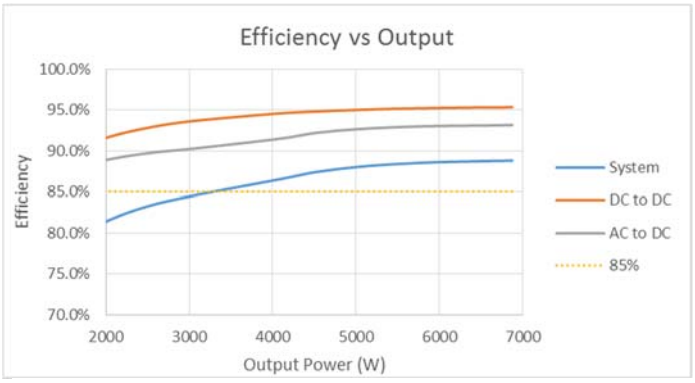

Figure 8: Symmetric Coils - Test conditions for efficiency and output included an 88 kHz switching frequency, a 525V AC/DC supply, concentric coils with a 21 cm separation and 360-volt output load voltage.

Bench evaluations of the system led to several design enhancements and revisions to both the transmitter and receiver with a drastic reduction of the physical dimensions and upgraded components, including an asymmetric coil.

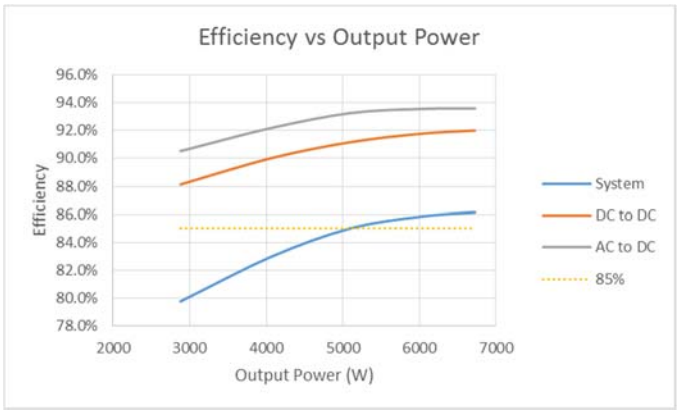

Figure 9: Asymmetric Coils - Test conditions for efficiency and output included a switching frequency of 87 kHz, a 525V AC/DC supply, greater than 20 cm coil-to-coil separation and an output load of 360V.

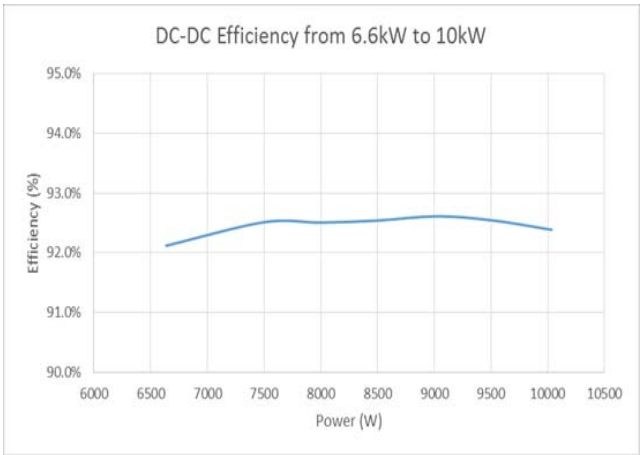

Figure 10: Asymmetric coil efficiency data at higher powers.

Test conditions for charting DC-to DC-efficiency included 87 kHz switching frequency and a 480V AC/DC supply to reach higher power levels. Output power was limited by the electronic load used. Higher power was achievable by connecting two loads in series.

A custom boost active power factor controller (PFC) board was built to provide DC voltage to the wireless charging transmitter, However, the custom PFC did not work, so Mojo continued to use the off-the-shelf unit to provide DC voltage. In Phase II, a new PFC was designed and built which worked well and demonstrated very high overall system efficiency.

Embedded control firmware was architected and written to support the system. It was debugged using off-the-shelf evaluation modules from microprocessor vendors, allowing development without actual hardware while awaiting full system integration. The firmware was tested with acceptable results on the actual system at lower power levels in the third quarter of 2013.

A second demonstration of the WPT system performance via hardware test with DOE observers in September 2013 successfully met the Phase I go/no-go requirements to continue the project, including fully charging the usable capacity of the vehicle battery.

Coils and magnetics were designed and tested against the electromagnetic simulation data on the new electrical hardware. A larger charger coil was constructed and tested at up to half the go/no-go power transfer criteria with preliminary efficiencies measured in the expected range.

A test fixture for coil misalignment was designed in which the receiver coil is mounted to a XYZ linear stage and can be positioned through computer control to achieve whatever misalignment position is desired. This test fixture helped in alignment testing and demonstration.

The greatest Phase I accomplishment was constructing a fully functional prototype wireless power transfer system. That included demonstrating fully operational complex PCBs in a live wireless power transfer environment at medium power outputs, and demonstrating embedded firmware control of a wireless power system in a live environment.

The team conducted measurements of electromagnetic fields comparable to computer-simulated results, and gained a better understanding of the project requirement constraints, how to choose components and material, and what system geometry and functional architecture should be constructed.

Phase II: Technology Implementation

The project team conducted a detailed review of target mechanical and electrical requirements on the Kia Soul EV to be used as a surrogate vehicle. Hardware, coil, magnetics and firmware were upgraded before a third prototype system was developed using the same Phase I go/no go criteria.

Vehicle integration and testing of hardware, coil, magnetics, and firmware development for Controller Area Network (CAN) and interlock interfaces between the charger and the vehicle was completed.

Critical tasks in Phase II technology implementation included the evaluation of vehicle integration issues, including a detailed review of target EV mechanical and electrical requirements; draft hardware, coil, magnetics, and firmware system requirement standards for wireless communications.

Following completion of the much smaller second revision of the Tx and Rx boards, the larger of the two candidates for a final vehicle integration coil set was chosen to ensure proper coupling. An on-vehicle system packaging location on the Kia Soul was defined.

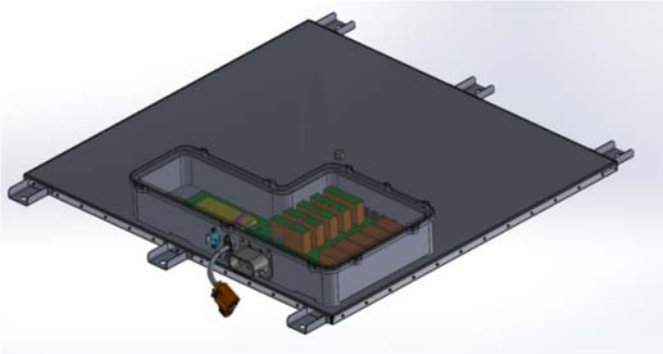

Figure 11: On-vehicle coil and electronic control unit.

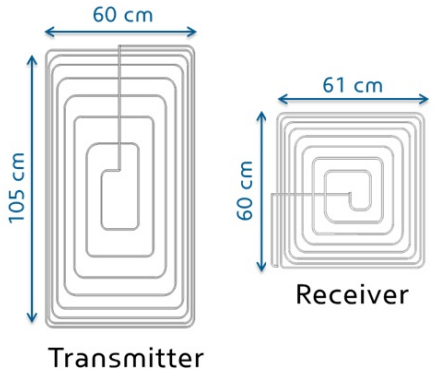

Figure 12: Transmitter (Tx) and Receiver (Rx) coils.

Initial testing results for the second-generation boost power factor correction (60 Hz AC-to-DC Converter) showed the unit could function at nearly 98 percent efficiency. The on-vehicle system architecture was determined and exterior dimensions were established.

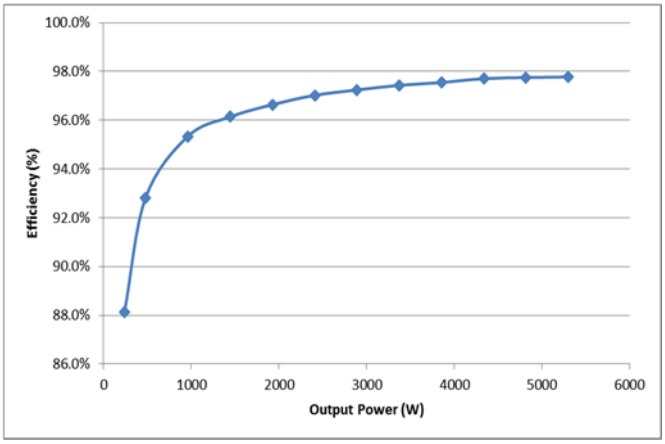

Figure 13: Phase II Power Factor Control.

The second-generation boost power factor correction (60 Hz AC-to-DC converter) showed the unit could function at nearly 98 percent efficiency.

Complete integration of the third-generation Tx and Rx module featured boards and housing designed with drastically reduced physical dimensions compared with the second generation. This resulted in a 3 percent efficiency increase. The third-generation wireless charging system was mechanically integrated onto the Kia Soul surrogate vehicle and demonstrated for DOE observers on May 27, 2015.

At that time, the charger-to-vehicle communications were not functioning correctly so the demonstration was performed using an electronic load. In Phase III the system was demonstrated again with full functionality and charged the Kia Soul EV battery. Measurements showed power transfer exceeding 6.6 kW with better than 85 percent efficiency and a vertical gap of greater than 20 cm.

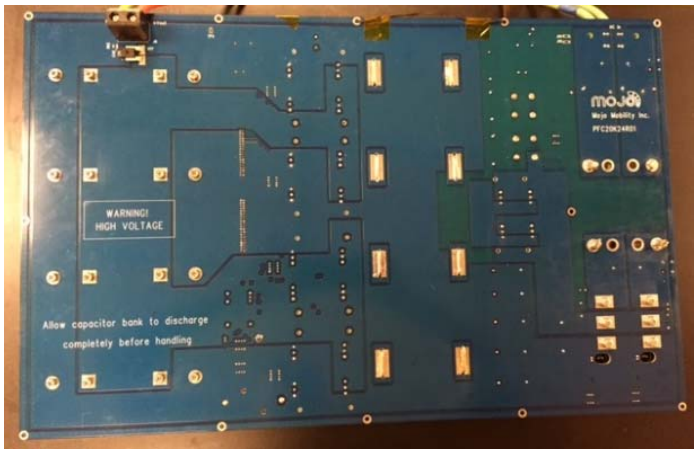

Figure 14: High Efficiency (98%) AC/DC Power Factor Correction (PFC) front end. The design and fabrication of the first-generation boost power factor correction (60Hz AC to DC Converter) was completed and tested at 10kW. It featured 240V AC input with capacitors that helped Smooth conversions of the current to 480V DC output. The small volume design (63 x 40 x 13 cm) was constructed on a single PCB with micro-controlled with firmware for startup, control of stand-by power and interface with the transmitter.

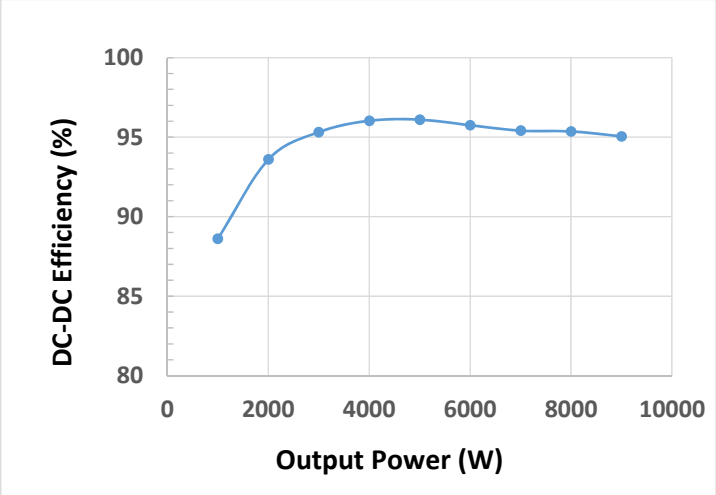

Figure 15: Phase II System DC-DC Efficiency from 1kW to 9kW. Phase II X-Y positioning was smaller than Phase 1 but sufficient for most applications greater than +/-20 cm. Output power was limited by electronic load but higher power was possible with two loads in series.

During the completion demo, one of the field effect transistors (FETs) on Power Factor Connection (PFC) failed due to a design issue in the boost inductors used whereby the inductor core saturated at high currents and changed the inductor characteristics. The PFC was improved by switching the custom inductor manufacturer to MPS Industries and testing and validating the inductors at the operating current.

Phase II accomplishments included the mechanical integration of the complete third-generation wireless charging system into the Kia Soul EV surrogate after an in-house design of the complete wireless charging system and the second-generation AC/DC front end.

Commercial Potential

Navigant Research was commissioned by HATCI to conduct a Cost Analysis and Commercial Viability Study in the second quarter of 2015 as part of Phase II. The study covered cost assumptions, consumer acceptance, petroleum reduction benefits from wireless charging, and commercial potential.

HATCI provided Navigant with the bill of materials (BOM) from its current-generation prototype wireless charger. Navigant sought pricing on 370 unique components listed on the BOM, not including Ferrite tiles, coil and magnetics and capacitors. Navigant determined the pricing for building 1, 1,000 and 50,000 systems.

Production Level	Unit Cost
1 unit	$8,981.01
1,000 units	$7,404.46
50,000 units	$7,141.04

Table 1: 2015 pricing for Hyundai wireless chargers.
Source: Navigant Research

It would be less expensive to make 50,000 units versus 1,000 units by integrating some parts into custom components that could be manufactured at volume which would save money thus eliminating the need to purchase individual parts. Large scale integration would bring the price down quickly, but the curve would flatten out. By 2021, the price of wireless chargers are expected to fall from an estimated $8,000 to $2,800 retail.

Reducing costs through engineering has cut the price of residential conductive chargers to the point of becoming a conventional commodity than a specialty item. The prices range from around $600 to $800 and are expected to fall to around $450 by 2020. [Jerram, L., Gartner, J., & Abuelsamid, S. (2015). *Wireless Charging Commercial Viability Analysis* (p. 4, Publication). Navigant Research.]

These chargers are capable of power transfer of up to 6.6 kW or 7.7 kW. However, such AC chargers essentially consist of a ground fault-tolerant circuit breaker and some communication circuitry to communicate with the EV. The AC-to-DC conversion occurs in the vehicle's on-board charger, which is included with every EV. These on-board chargers are typically limited to 7 to 10 kW and charging at higher rates would require more sophisticated and expensive DC fast chargers. The HATCI wireless charging system is designed to operate at up to 19.2 kW. A comparable wired fast DC charger may be comparable in price at high volumes.

Because of the scarcity of wireless charging, it is likely that vehicles equipped for wireless charging will still need conductive charging capabilities for some time to come.

Overall, wireless charging remains largely a pre-competitive market. Nearly every major plug-in vehicle manufacturer is at some stage of developing or licensing a wireless charging system for their vehicles. Navigant Research reported that early interest in wireless charging is coming from premium automakers whose customers may be more willing than other plug-in electric vehicle (PEV) drivers to pay more for wireless charging at home. [Jerram, L., Gartner, J., & Abuelsamid, S. (2015). *Wireless Charging Commercial Viability Analysis* (p. 6, Publication). Navigant Research.]

The best route to market success for a wireless charger is an OEM developing a charger that can be integrated into its own PEV models, whether developed in house or through a partnership with a technology company.

Current wired DC fast chargers range in efficiency from 85 percent to around 93 percent today. A well-designed wireless charging system as described here can have comparable efficiencies. The reason for this is that the main components of the two systems are comparable. They both include a PFC and DC-DC converter and a transformer. In the case of the wireless charger, the transformer consists of the Tx and Rx coils and also performs the DC-DC conversion. With a well-designed magnetic system allowing high-efficiency coil-to-coil power transfer, the wired and wireless charging systems can achieve comparable efficiencies.

While up to 50 percent of PEV buyers are content to use the Level 1 cord set that comes with the vehicle, a higher percentage of battery electric vehicle (BEV) owners purchase Level 2 chargers capable of delivering power from 6.6 kW to 20 kW.

Navigant's view is that 6.6 kW will be the minimum power delivery for wide adoption of wireless charging systems. [[Jerram, L., Gartner, J., & Abuelsamid, S. (2015). *Wireless Charging Commercial Viability Analysis* (p. 7, Publication). Navigant Research.]

The primary advantage of wireless charging over cabled connections is ease of use and avoiding cord management issues, such as trip hazards. The convenience is a combination of simply parking a car and walking away as a driver does with a conventional gasoline-powered vehicle.

Overall, Navigant projects the North American residential electric vehicle supply equipment (EVSE) market will likely grow from an estimated 138,000 units in 2015 to about 638,000 in 2024. Wireless chargers could account for around 6.5 percent of the market barring a significant breakthrough that would make wireless charging preferred over connected charging. [Jerram, L., Gartner, J., & Abuelsamid, S. (2015). *Wireless Charging Commercial Viability Analysis* (pp. 11-12, Publication). Navigant Research.]

Two factors could shift the forecasted demand for wireless residential charging. If wireless charging takes off in the commercial charging market, it could spur greater demand in the residential market, as drivers will already be accustomed to wireless charging in public spaces and would seek wireless home charging as well. The balance toward wireless charging could also shift if one automaker made wireless charging its only option for EVs. Navigant says this is unlikely in the early years of wireless charging because of the lead that connected charging has in public infrastructure.

Navigant estimated the petroleum displacement that would occur as a result of PEVs using wireless charging between 2015 and 2024. Assuming 11,000 average annual miles of driving, PEVs charged with wireless units were expected to displace 120,000 gallons of petroleum-based fuel in 2015 rising to 76,131,000 gallons of a cumulative displacement of 241,482,000 gallons by 2024. [Jerram, L., Gartner, J., & Abuelsamid, S. (2015). *Wireless Charging Commercial Viability Analysis* (p. 14, Publication). Navigant Research.]

Commercialization of the HATCI advanced wireless power transfer system would provide the public with a high-efficiency, low electromagnetic interference (EMI) and a positioning tolerant alternative to Level 2 conductive and Level 3 direct current (DC) fast charging, both of which present a tripping hazard because of charging cords.

Phase III: Technology Demonstration

In Phase III, four additional Kia Soul EVs and wireless power transfer charge stations were developed and demonstrated in real-world conditions. Independent testing at Idaho National Laboratory (INL) and at HATCI was conducted. One vehicle and wireless charging system was provided to the DOE for testing. In parallel with the demonstration, refinements were identified for additional work.

The goals for Phase III technology demonstration included design improvements to address issues found in Phase II and to improve safety and reduce cost.
These improvements included new gate drivers and field effect transistors (FETs) in the fourth-generation transmitter, and the substitution of ferrite tiles as a covering for the transmitter. This represented a 90 percent cost saving and provided the same performance as previously used material.

On the communications side, integrating real-time operating system (RTOS) software resulted in a faster response, more robustness and reduced the system's susceptibility to communications disruptions and delays. A decision was made to run in parallel Wi-Fi, CHAdeMO communications and a proportional integrated derivative controller (PID). The fast-charging DC CHAdeMO communication software module within the receiver's Electronic Control Unit (ECU) was fully established and tested.

For the fourth generation WPT, discrete metal-oxide semiconductor field-effect transistors (MOSFETs) were used in place of a power module for an H-bridge circuit that enabled voltage to be applied across a load in the opposite direction in the resonant inverter.

This improved thermal characteristics to 1800W maximum power dissipation from 312W, and each FET had its own heat sink. It also provided easy assembly/disassembly at about a 40 percent cost reduction. A Beagle Bone Linux system was incorporated for remote diagnostics.

New gate drivers for MOSFETs incorporated galvanic isolation to separate electrical circuits and block stray currents. The result was higher drive current capability with no other components needed. Added safety features included under voltage/overvoltage protection, the insertion of high-side low-side dead time, the time after each event when the system is unable to record another event. Temperature shutdown and surge protection were added to the AC/DC converters.

The redesign of the full bridge resonant converter geometry kept the phase shift to a smaller resolution (0.03º) in high-resolution pulse width modulation (PWM), or digital mode. The Rx received CHAdeMO messages and sent them to the transmitter via Wi-Fi. The PID control helped to make a stable system for all ranges of voltages even with Wi-Fi delays and non-linearity challenges. The new methodology implemented allowed different parameter sets as the digital phase shift change and current responded to varied output voltages.

Prior to interface with the battery, the coil, magnetics and power electronics worked well, delivering total system (grid to DC output) efficiency of 93 percent at greater than 6.6 kW while the custom AC/DC front- end delivered 98 percent efficiency at power transfer up to 10 kW.

A change to the timing of the control signals in the communications software ensured the correct messages were being sent and deciphered at the appropriate times. That allowed a first attempt at charging the vehicle through wireless power.

However, before power was ramped up, more stability issues were identified. The communication between the charger and user control PC was disrupted when higher voltage was applied to the system. This problem was traced to electromagnetic interference (EMI) with the transmitter inverter board. Magnetic fields from the coupled coils were also suspected.

Even when the communication was working, the mouse pad on the laptop worked intermittently. This issue was solved by using a Wi-Fi link between the charger and PC instead of a wired connection. Shielding was added to a portion of the transmitter board which was suspected of being subject to EMI disruptions.

With some of the technical issues resolved, the EV battery was successfully charged from a test fixture with wire harnesses functionally connected to the vehicle for charging at 7.0 kW, resulting in 94 percent DC-DC efficiency. Further refinement led to closed-loop control using a hard-wired communication link for wireless power transfer between the transmitter and receiver. The closed-loop current control worked in parallel with vehicle-charger communications and the time of charge was satisfactory without faults.

When the receiver was mechanically mounted to the vehicle, the Wi-Fi communication between the transmitter and receiver was unstable and signal strength was significantly reduced because of the conductive structures surrounding the receiver Wi-Fi antenna. The Wi-Fi link was improved somewhat by changing the antenna on the transmitter side and amplifying the antenna to boost transmitted signal strength.

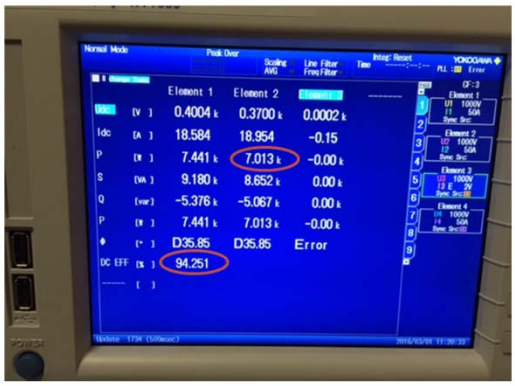

Figure 16: Power analyzer showing output and DC efficiency.

Testing Plan

Voltage and current measurements at the system input and output and instrumentation to measure temperature at the top surface of the ground Tx assembly, the Tx and Rx coils and the battery locations were established.

The Kia diagnostic instrument was connected to the vehicle to monitor battery management system (BMS) data, such as battery voltage, current and state of charge (SoC). Water and oil and a selection of foreign objects were placed between the Tx and Rx assemblies to simulate the effect on wireless power transmission at the z-gap height of 20 cm.

Obstruction Element	Description
No obstruction	Tx assembly is dry and free of oils, fluids and foreign objects
Water	Water sprayed over Tx assembly to simulate rain and snow on pavement
Motor Oil	Motor oil sprayed over Tx assembly to simulate spill of fluid other than water
Foreign Objects	Soda can or other object laid on top of Tx assembly

Table 2 - Obstruction elements used in testing.

Continuous measurement of voltage, current and power were taken at the vehicle ground Tx assembly input and vehicle Rx assembly output to calculate power efficiency from the main AC power supply to the battery. Power efficiency remained at 85 percent or above and continuous measurement of the WPT power factor during charging remained above 0.90.

	Battery	Primary Tx Unit Input	Secondary Rx Unit Output
Voltage	240-413VDC	240VAC+/-10V	240VDC – 413VDC
Current	13A-30A	22A-40A	13A-30A
Power	6.6 kW+/-1 kW	5.6 kW – 9.1 kW	6.6 kW+/-1 kW

Table 3 - Acceptable range of values for voltage and current at the three locations.

A physical switch on the main AC power supply was installed to cut power in case of a system malfunction or abnormality that could damage the WPT system, the vehicle, surrounding property or harm any people in the vicinity. The test engineer used both electric and magnetic field probes to gauge EMC and EMF emissions levels as needed. The engineer also was required to stay far enough from the WPT system so that emissions levels were below the 2010 ICNIRP thresholds at 85 kHz.

The basic performance test procedure was conducted for all four obstruction conditions at five different alignments, including one that simulated roll, pitch and yaw of the vehicle Rx assembly along the vehicle (X) and laterally (Y).

The battery was tested at 50 percent state of charge (SoC) +/- 2 percent and the vertical distance between the primary and secondary coil was equal to 20 cm. Voltage, current, power and temperature were constantly measured. Wireless charging started at 6.6 kW and continued until the system automatically shut off. The battery was then discharged to 50 percent +/- 2 percent to prepare for the next test.

To determine electrical performance of the Rx assembly, the test engineer powered up the Tx assembly and used a debugging tool to monitor the Wi-Fi connection between the two modules. Supply input voltage to the Rx module varied between 11V and 14V. A pass was determined if there was no interruption to the Wi-Fi.

Varying input power between 200 Volts AC (VAC) and 260 VAC to the front end Power Factor Control with a 6.6 kW load and 480 Volts DC passed if the system operated normally with no interruption or reduction in output power or voltage.

To emulate electrical grid performance, a voltage spike higher than the nominal 240 VAC was administered. The pass criteria required no permanent damage to parts.

Due to the high voltage present in the system and the dangers posed to the development of this type of system, all Mojo Mobility employees attended an electrical safety class. Special steps were taken to make sure the lab development environment was safe.

Idaho National Lab Testing

Independent testing of the Kia Soul EV with the complete WPT system began in May 2016 at the Idaho National Lab (INL). The initial power up was interrupted by the INL's emergency stop safety module. Investigation revealed that radiated emissions from the wireless charging system were coupling with low-voltage electronics in the emergency stop module, causing the emergency stop to behave erroneously. INL removed some unnecessary electronics from the emergency stop module and testing continued.

However, before INL could complete the full testing plan, the wireless charging system failed and was returned to HATCI, where INL's data from one week of testing and a physical inspection of the PCB suggested the failure was due to operating in very low-efficiency conditions. Too much power was being dissipated in the invert MOSFETs, eventually causing some of them to fail. Along with the inverter board, the PFC also failed.

A Redesign of the charger electronics hardware and software were made before testing resumed at INL. The redesign made it immune to voltage interruptions, and it automatically shut off in case of abnormally low-efficiency conditions.

The failure at INL also exposed weaknesses in the system design and increased the understanding of inverter MOSFET switching conditions, which are called hard switching and zero-voltage switching (ZVS).

Another weakness in the system learned from INL testing was high EMF radiation levels well beyond the International Commission on Non-Ionizing Radiation Protection (INCIRP) safety limits. Further research is needed to determine the best solution to lessen the electromagnetic fields. [ICNIRP 2010 Electromagnetic Field Guidelines. (2015, December 31)]

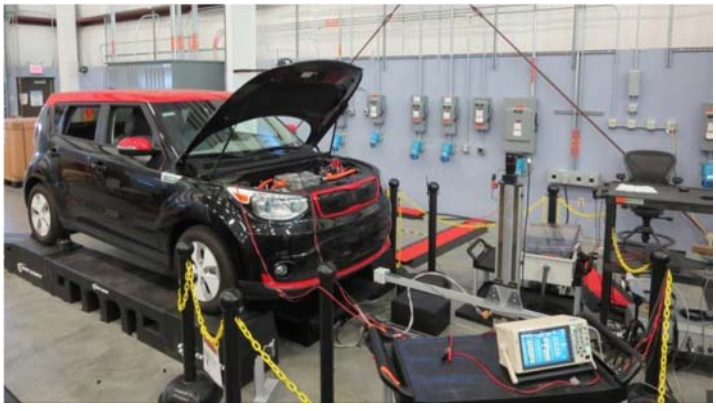

Figure 17: Idaho National Lab setup.

The prototype 85 kHz wireless charging system in the surrogate 2015 Kia Soul was designed and developed to be capable of up to 19.2 kW output over a 20 cm coil-to-coil z-gap, with more than 90

percent system efficiency. The system is also capable of operating at gaps ranging from 150 mm to 210 mm.

The coil size depends on the maximum power transfer level requirement. While the HATCI WPT system was designed for up to 19.2 kW output, the coil size would be reduced for a lower power target. Both the transmitter and receiver coils use Litz wire, which carries alternating current, and has a 2 mm layer of ferrite (N95 material) covering the complete coil area to improve efficiency and reduce radiated EMF emissions.

Figure 18: Receiver coil set in coil housing.

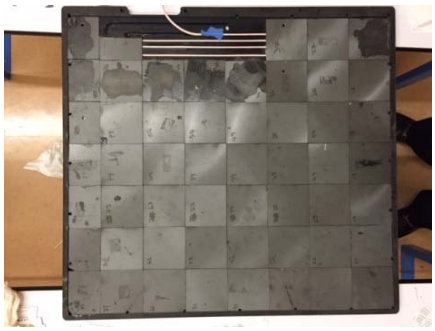

Figure 19: Receiver coil set with inset ferrite tile layer.

The WPT system was demonstrated up to 10 kW output when aligned and at nominal ground clearance. Charging at 19.2 kW may be pursued in future projects. INL testing operated the WPT up to a charge power level of 7.0 kW output which is more closely aligned with industry standard levels.

The INL test setup was made up of a servo-motor driven, coil-positioning system that accurately positioned the ground coil assembly (Tx) with respect to the vehicle coil assembly (Rx) to within +/- 0.2 mm. This allowed the coil positioning system to operate with misalignment up to +/- 30 cm along the side (x-axis) of the vehicle and along the front (y-axis) in front of the vehicle. The coil-to-coil height (z-gap) was set to handle a separation of up to 27.5 cm.

To accommodate the overall height of the coil positioning system under the WPT, 35 cm ramps were used to elevate the vehicle for testing. They contained no metallic or conductive components and therefore had no impact or interaction with the electromagnetic field (EMF) created by the WPT system during operation.

A high-accuracy four-channel power meter, a data acquisition system and an EMF measurement probe were used to measure EMF safety, power quality, and performance efficiency capabilities of the WPT system. The power meter measured electrical power at multiple nodes throughout the WPT system to determine the overall system AC to DC efficiency and sub-system efficiencies. It also quantified the power factor and the total harmonic distortion (THD) from the electric grid. The EMF measurement probe quantified the magnetic and electric fields and measured the lowest frequency produced by the WPT system.

The data collected was used for in-depth analysis and to visualize performance and safety metrics across the range of testing conditions.

When INL testing resumed in late 2016, a wide range of coil misalignment, coil gap and power transfer levels were covered. Measured values included overall AC-to-DC system efficiency, sub-system efficiencies, power quality metrics, and EMF radiation emissions around the vehicle.

Nominal operating conditions for the WPT system were defined as 7.0 kW DC output with the coils in alignment and a coil-to-coil z-gap of 20 cm. Dividing total DC output power by the total grid AC input power drawn by the WPT system resulted in total system efficiency of 88.4 percent.

Front-end power electronics efficiency was 96.5 percent, based on calculations that included the power factor correction circuit and fans, lights, and communications controls devices.

DC-to-DC efficiency was 91.7 percent based on dividing the DC output power provided to the vehicle's high-voltage DC bus by the DC output from the power factor correction (PFC) circuit. The PFC included the full bridge resonant inverter, the resonant tuning circuit, the coil-to-coil coupling, and the output rectifier with smoothing circuit.

The magnetic and EMF measurements of 18.3 amps per meter (A/m) and 278 volts per meter (V/m) were recorded with the WPT operating at 7.0 kW. Both exceeded the 2010 ICNIRP safety guidelines. The EMF probe was positioned about 20 cm from the front surface of the vehicle (y-gap), along the center line of the vehicle (x-gap) and the vertical (z-gap) between the transmitter (Tx) and receiver (Rx) – much closer than most humans would stand.

Coil-to-coil misalignment and coil-to-coil gap are primary factors influencing WPT efficiency. To quantify impact of coil-to-coil misalignment along the x-axis (fore to aft of the vehicle) and y-axis (side to side) on the total system efficiency of the WPT, a full range of testing was conducted to detail the total system efficiency.

As expected, the peak efficiency of 88.4 percent occurred where the coils were in magnetic alignment. Misalignment in either the X or Y direction resulted in a decrease of total system efficiency. The reduction in system efficiency was greater in the y-axis for a given coil-to-coil misalignment, primarily due to the non-square coil assembly design of the WPT system. Dimensions along the x-axis of the ground assembly (Tx) and the vehicle assembly (Rx) were 92 cm and 80 cm respectively. Dimensions along the x-axis were 118 cm and 74 cm respectively. This resulted in a ground coil assembly to vehicle coil assembly overlap of +/-6 cm along the y-axis and +/-22 cm along x-axis.

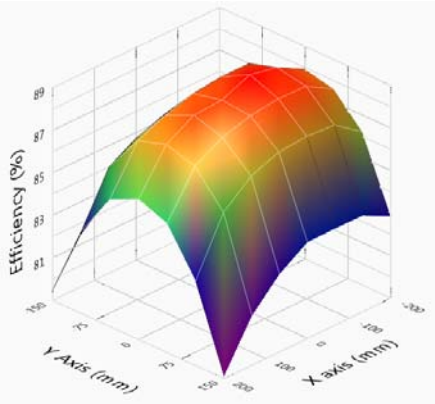

Figure 20: Coil-to-coil misalignment measurements. Total system efficiency (AC to DC) when operating at 7.0 kW output power and a coil-to- coil gap of 200m across a range of x and y coil-to-coil misalignments.

During WPT testing, the power was measured at multiple points along the path of power flow, enabling analysis of sub-system efficiencies of various components within the WPT as well as quantifying the total system efficiency.

Two sub-system efficiencies were analyzed for this testing – front-end power electronics efficiency and DC-to-DC efficiency. The analysis provided insight as to the mechanisms of WPT system power loss. Testing was conducted across the x-axis at coil gaps of 150 mm, 175 mm and 200 mm to quantify the impact of changes in the coil-to-coil gap and the impact of x-axis misalignment on total system and sub-system efficiencies.

Testing across a range of the same three coil-to-coil misalignment gaps along the vehicle side-to-side y-axis showed the front end power electronics sub-system efficiency was nearly constant across the y-axis misalignment with a small increase in efficiency as the coil gap decreased.

By contrast, the DC-to-DC sub-system efficiency was reduced by 4 percent at a +/-150 mm misalignment along the y-axis and showed a nearly symmetrical trend. This was a significantly greater impact in the y-axis misalignment compared to the x-axis misalignment of +200 mm, which resulted in a 1.5 percent reduction. The coil-to-coil gap also impacted DC-to-DC sub-system efficiency with a variation of greater than 2 percent.

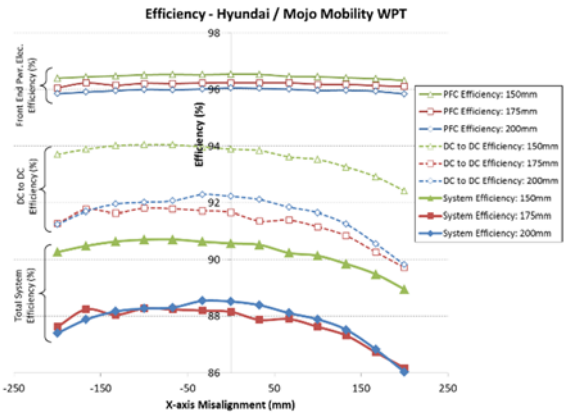

Figure 21: X- misalignment testing for three coil-to-coil gaps. The front-end power electronics sub-system efficiency was nearly constant across the range x-axis misalignment, but had a small increase in efficiency when the coil gap decreased from 200 mm to 150 mm.

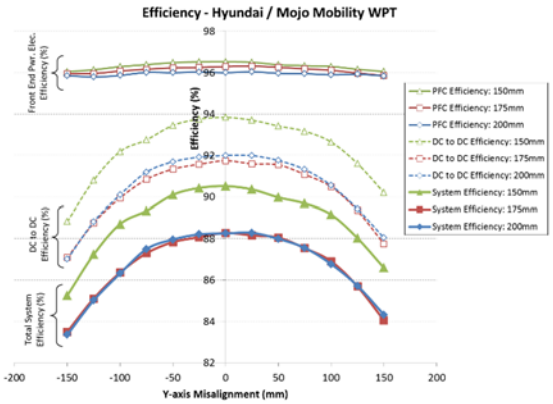

Figure 22: Y-misalignment for three coil-to-coil gaps tested. DC-to-DC sub-system efficiency was reduced by 4% percent at a +/-150 misalignment along the y-axis and showed a nearly symmetrical trend.

The DC-to-DC sub-system efficiency was negatively impacted by misalignment as well as showing a non-symmetrical trend from the positive-to-negative misalignment.

A misalignment of +200 mm, where the ground coil assembly was farther under the vehicle, resulted in 1.0 percent to 1.5 percent lower DC-to-DC subsystem efficiency than a misalignment of -200 mm, where the ground coil assembly was less covered by the vehicle.

The change in coil-to-coil gap from 200 mm to 150 mm had a significant impact on the DC-to-DC sub-system with a variation of greater than two percent change in efficiency. These results showed the DC-to-DC power transfer accounted for the majority of the loss during charging.

Additionally, the DC-to-DC efficiency showed the greatest impact from both misalignment as well as coil-to-coil gap, indicating the change in the magnetic coil-to-coil coupling significantly contributed to the change in efficiency. Overall the total system efficiency ranged from 86 percent to over 90 percent across the range of misalignment and coil-to-coil gap tested.

The total system efficiency, comprised of the two sub-system efficiencies, showed a symmetrical trend for efficiency across misalignment along the y-axis. Overall, the total system efficiency ranged from less than 84 percent to greater than 90 percent across the range of misalignments and coil-to-coil gaps.

Throughout all phases of testing, the power meter was used to measure the quality of the WPT system input power to determine the interaction and influence of the WPT system on the electric grid-supplied power. From these measurements, the power factor and the input current total harmonic distortion (THD) of the WPT system were determined.

Across the various test conditions, such as coil-to-coil gap and misalignment, the power factor and input current THD were very consistent. However, at reduced power levels there was measureable change in both the power factor and THD.

The best power factor and input current THD occurred at full power transfer and was measured to be 0.995 power factor and 9.5 THD percent respectively. As power transfer decreased, the power factor also decreased and the THD increased. The results showed no significant influence of coil-to-coil gap on power factor or THD. Overall test results showed the power factor exceeded the industry minimum limit of 0.95.

Electromagnetic Field (EMF) measurements were conducted during a complete cycle charge test at the front of the vehicle in a precise grid pattern to characterize and visualize the EMF magnitude next to the front bumper of the vehicle. The center of the EMF probe was positioned at grid locations ranging from -200 mm to +650 mm in the z-gap direction and from -450 mm to +450 mm in the y direction. For all measurements, the center of the EMF probe was positioned 200 mm from the forward-most surface of the vehicles front bumper.

EMF emissions around the WPT system at the front of the vehicle slightly exceeded the ICNIRP 2010 public exposure limit. With the EMF probe placed in the gap between the transmitter and receiver, the highest electric field measured was 425 V/m, or more than five times the public exposure limit of 83 V/m. These measurements exceeded the scope of DOE requirements.

The HATCI WPT system operated at a constant fundamental frequency of 88.3 kHz across all test conditions including misalignment and variation in coil-to-coil gap. The system demonstrated high efficiency, high power quality, and overall low magnetic field emissions.

Total AC-to-DC system efficiency at the nominal coil-to-coil gap of 20 cm ranged from 80 percent to a peak efficiency of 88.4 percent when aligned. With a decreased coil-to-coil gap of 150 mm, total system efficiency exceeded 90 percent.

Overall, the independent test results exceeded HATCI project goals of greater than 85 percent efficiency, greater than 6.6 kW charging capability and 20 cm coil-to-coil lateral misalignment while meeting regulatory guidelines.

Test	Results
Ground clearance (coil gap)	200 mm
Total system efficiency (AC to DC)	88.4%
Front-end power electric efficiency	96.5%
Magnetic field at front of vehicle	18.3 A/m
Electric field at front of vehicle	278 V/m
Input current- total harmonic distortion (THD)	9.5%
Input power factor	0.995
Operating frequency	88.3 kHz

Table 4: Idaho National Laboratory independent test results.

HATCI Testing

In the third quarter of 2016, while independent INL testing was under way, HATCI began extensive testing on the wireless charging system in ideal and abnormal operating conditions. Tests included:

- Roll and Pitch of the transmitter at +/- 15 degrees.
- Foreign Object Detection to determine rising temperatures and when they stabilized.
- Electromagnetic Field Emissions (EMF) to determine compliance with international guidelines for human exposure.
- Electromagnetic Compatibility (EMC) to measure radiated and conducted emissions during active power transfer.

Figure 23: Phase III durability setup at HATCI.

Test equipment included a vehicle hoist for magnetic gap manipulation, a Yogogawa Power analyzer for voltage, current, power factor and efficiency measurements (with clamp-on current probes for higher accuracy.) A Narda EHP-200A E&H Field Meter was used to measure electric and magnetic fields and a thermal imaging camera was used to identify potential component failures. A DC power load and power supplies, oscilloscopes and temperature sensors were also used.

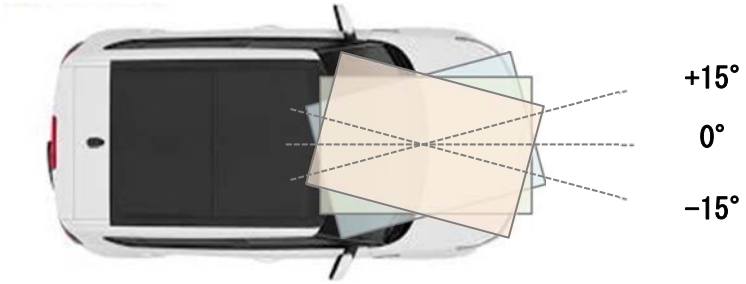

Figure 24: Coil rotation test.

To determine the effect of coil rotation on performance, the transmitter coil (Tx) was rotated 15° with the receiver (Rx) unchanged. The result was less than a one percent drop in efficiency. From September 2016 to February 2017, charging efficiency during pitch-and-roll testing improved by about 3 percent to better than 89 percent.

Rotation around X-Axis				
Power	Z-Gap (cm)	Height(cm)	Degrees	Effeciency
6.8 Kw	19 cm	2.54	2.18	90.70%
		5.08	4.34	91.00%

Rotation around Y-Axis				
Power	Z-Gap (cm)	Height(cm)	Degrees	Effeciency
6.8 Kw	19 cm	2.54	1.26	90.60%
		5.08	2.56	91.10%
		7.62	3.78	91.50%

Table 5: Results of transmitter rotation around front (x-axis) and side (y-axis) of vehicle

Testing was performed on the detection of foreign objects intruding on the electromagnetic field similar to what can happen in real-world wireless charging. An aluminum can with water reached 33.2 centigrade after eight minutes. An empty aluminum can reached 53C after the same time. An iron ruler placed between the transmitter and receiver generated the maximum temperature recorded, reaching 85.4C after eight minutes.

None of the objects significantly impacted efficiency before or after being placed. In a production system, safety mechanics could be designed to detect very hot objects and automatically shut down the wireless power transfer.

EMF radiation testing at HATCI found that electric and magnetic field levels inside the vehicles satisfied SAE International requirements but were not satisfied from the ground to 40 cm and from the vehicle to 20 cm.

The transmitter temperature stabilized around 50.2C. The hottest observed part of the assembly was the area around the capacitor bank. The receiver temperature stabilized around 55.9C. The hottest observed part was the power electronics enclosure.

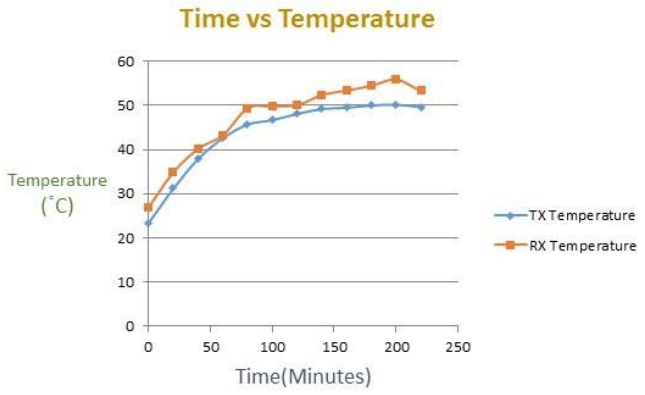

Figure 25: Transmitter (Tx) and Receiver (Rx) temperatures during complete charging cycle.

Various components around the charging system were observed with a thermal camera to identify hot spots. The hottest component was the left mounting bracket of the receiver assembly, which reached 82C after 161 minutes of charging. Other components remained at nearly room temperature.

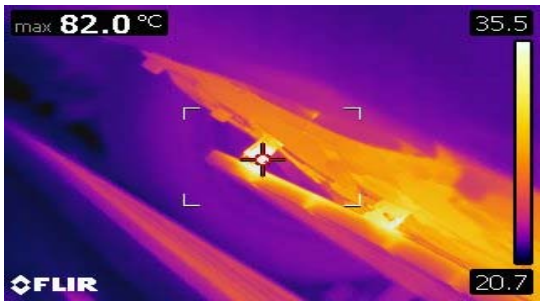

Figure 26: High heat affects left mounting bracket. A forward-looking infrared camera (FLIR) captured the heat signature of the receiver's left mounting bracket at 82C at 161 minutes of system charging.

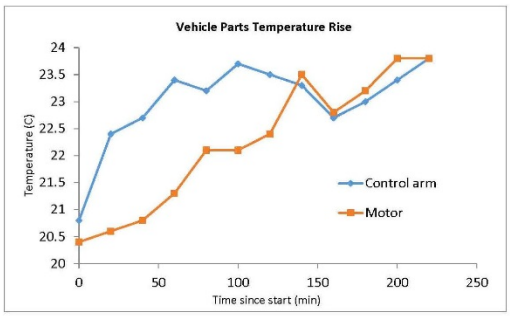

Figure 27: Most components around the receiver plate remained near room temperature.

EMC testing of the wireless charging system was conducted in December 2016 at Underwriters Laboratories (UL), where radiated and conducted emissions during active power transfer were measured against proposed limits in SAE J2954 TIR. Charging power was 6.8 kW with coils aligned at the center of the vehicle.

Radiated emissions measured were below the proposed SAE limit of about 1.3 megahertz (MHz) except for a spike to 2 megahertz (MHz), which exceeded the limit. Conducted emissions did not meet the SAE requirement. The frequency of about 88 kHz was within the SAE standard, however poor harmonics continued into the megahertz leading to excessive radiation.

It is believed that the emissions could be greatly reduced by designing a better filter at the output of the MOSFET H-bridge on the inverter circuit.

Total system efficiency during multiple complete charge/discharge cycles at 6.7 kW with a 20 cm z-gap between the transmitter (Tx) and receiver (Rx) remained consistent. After 210-220 minutes, overall efficiency was recorded at 87.2 percent, 87.4 percent and 87.5 percent in three runs. Peak efficiency of 90.3 percent came 20 minutes into the second run.

The thermal temperature of the transmitter (Tx) rose slightly higher in the third run to settle at 50.2C at 220 minutes after peaking at 51.6C at 180 minutes. The other runs were completed below 50C although the 200-minute reading during the second run touched 50C at 180 minutes and 50.2C at 200 minutes.

The thermal temperature of the receiver maxed out at 55.9C at 200 minutes of the second run and cooled to 53.3C at 220 minutes. The 5C spread between the first and second runs at 220 minutes was the biggest separation of any of the tests.

Overall Efficiency(%) @20 cm			
Time (min)	Run1 @6.7kW	Run2 @6.7 kW	Run3 @6.7 kW
20	90.0	90.3	90.1
40	89.7	90.0	89.7
60	89.5	89.9	89.7
80	89.3	89.9	89.6
100	89.3	89.9	89.5
120	89.3	89.9	89.4
140	89.2	89.9	89.4
160	89.1	89.8	89.4
180	88.9	89.9	89.3
200	88.8	89.8	89.2
220	87.2	87.5	87.4

Thermal Temp of TX (°C) @20 cm			
Time (min)	Run1 @6.7kW	Run2 @6.7 kW	Run3 @6.7 kW
20	30.4	31.2	31.8
40	36.8	37.9	37.4
60	43.5	42.6	42.6
80	43.8	45.7	46.6
100	44.0	46.7	48.0
120	45.7	48.1	48.8
140	47.4	49.2	49.7
160	48.3	49.5	49.9
180	48.7	50.0	51.6
200	49.1	50.2	51.4
220	48.3	49.8	50.2

Thermal Temp of RX(°C) @ 20 cm			
Time (min)	Run1 @6.7kW	Run2 @6.7kW	Run3 @6.7kW
20	30.4	34.9	35.2
40	36.8	40.2	40.3
60	43.5	43.3	44.1
80	43.8	49.4	49.7
100	44.0	49.8	49.8
120	45.7	50.1	51.1
140	47.4	52.4	52.3
160	48.3	53.4	53.6
180	48.7	54.5	55.0
200	49.1	55.9	55.2
220	48.3	53.3	50.1

Table 6: Total Efficiency and Temperature Charge/Discharge across three runs. Multiple full-charge cycle tests from about 5 percent to 94 percent state of charge at about 6.7 kW were run for 220 minutes showing stable performance over the charging range.

Time (min)	Overall eef. Percentage	PFC eff. Percentage	DC-DC eff. Percentage	Tx Temp. (°C)	Rx Temp. (°C)	Mounted Bracket (°C)
20	90.3	95.5	94.5	31.2	34.9	34.5
40	90.0	95.3	94.5	37.9	4.02	37.3
60	89.9	95.2	94.5	42.6	43.3	37.6
80	89.9	95.1	94.5	45.7	49.4	38.0
100	89.9	95.1	94.6	46.7	49.8	38.4
120	89.9	95.1	94.5	48.1	50.1	39.8
140	89.9	95.1	94.5	49.2	52.4	40.0
160	89.8	95.0	94.5	49.5	53.4	40.2
180	89.9	95.0	94.6	50.0	54.5	40.8
200	89.8	94.9	94.6	50.2	55.9	41.2
220	87.5	94.1	92.9	49.8	53.3	40.1

Table 7: Average Total Efficiency and temperature for 18 Runs Charge/Discharge.

What happens when two electric vehicles are wirelessly charging simultaneously when they are next to each other or positioned face to face? If wireless charging grows in popularity, multiple ground transmitters may be located near each other.

Testing at 20 cm and 40 cm height between the vehicles found both the electric and magnetic fields were below the 2010 ICNIRP standard for human exposure to radiated emissions. The transmitter (Tx) and receiver (Rx) temperatures were steady at about 30C. The average system total efficiency was about 90.2 percent and 90.4 percent.

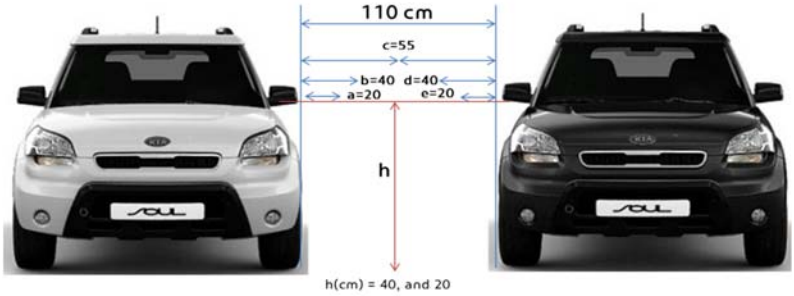

Figure 28: Side-by-side EMC compatibility testing.

Location	Electric Field(V/m)		Magnetic Field(A/m)	
	40 cm	20 cm	40 cm	20 cm
a	22.885	61.187	5.9947	4.3756
b	33.077	48.614	2.7415	2.0383
c	30.395	47.539	1.9048	2.5978
d	31.308	38.24	1.8287	2.5681
e	21.903	45.983	4.8344	3.5708

Table 8: Positional readings from electric field and magnetic field testing.

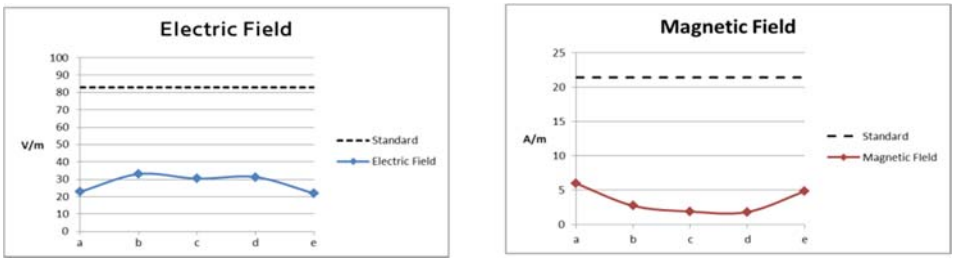

Figure 29: Electric and magnetic field at 40 cm.

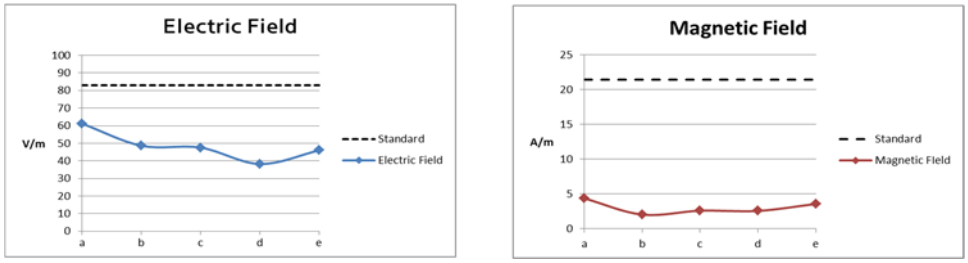

Figure 30: Electric and magnetic field at 20 cm.

In face-to-face EMC testing, the magnetic field is below ICNIRP guidelines for all test conditions. The electric field exceeds the limit when the probe is exposed directly to the field at a height of 20 cm. Total system efficiency for both vehicles was constant through the test, averaging 91.0 percent and 89.0 percent total efficiency.

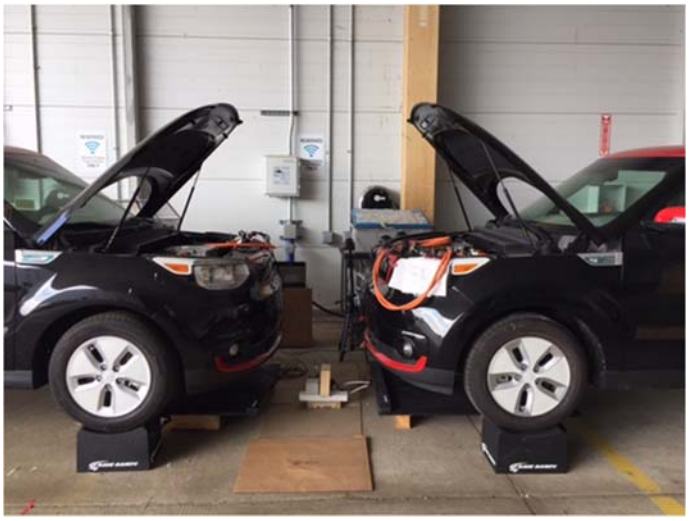

Figure 31: Face-to-face EMC compatibility testing.

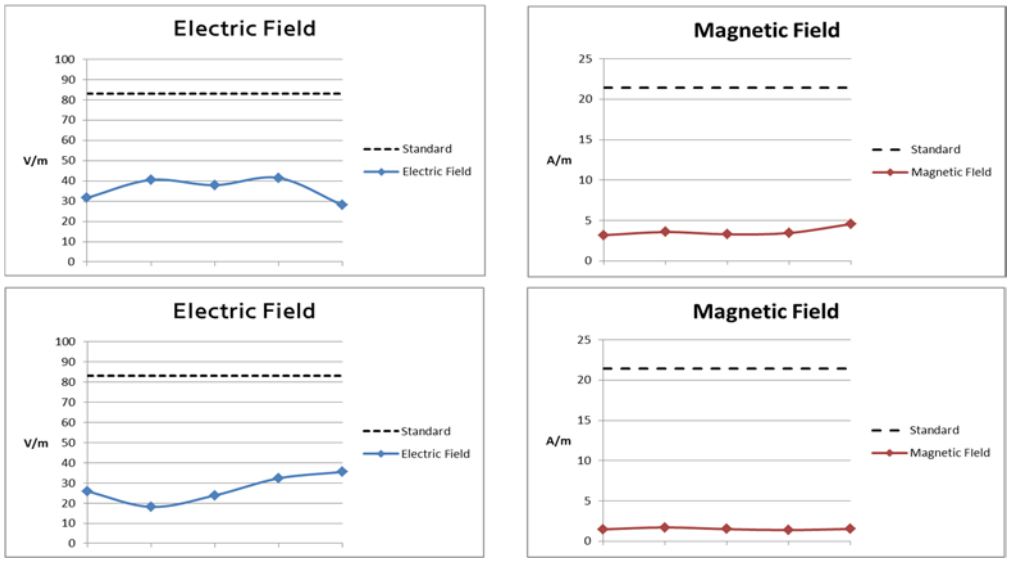

Figure 32: Comparison of electric and magnetic fields along the tire and along the driver center line.

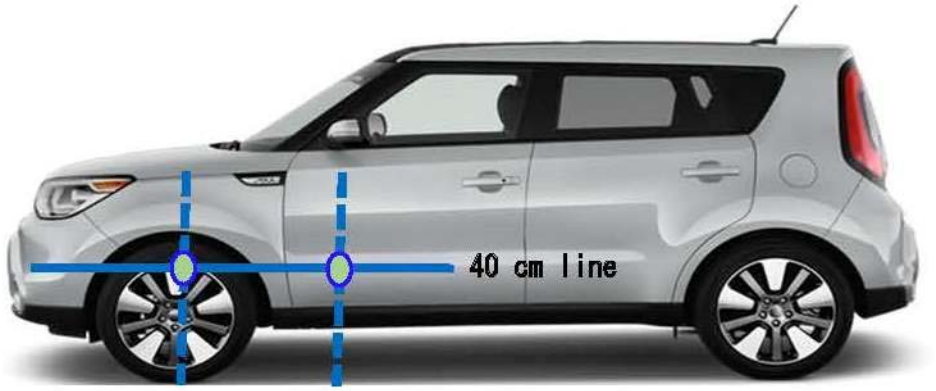

Figure 33: Height and centerline comparison at 40 cm.

The INL and HATCI testing revealed several issues and solutions incorporated into the project workflow. The chart below highlights the problems and solutions.

Problem	Solution
Communication between the charger and user control PC disrupted when higher voltage applied to the system	Using Wi-Fi link between charger and PC instead of wired connection. Shielding added to portion of transmitter board suspected of being subject to EMI disruptions
Initial power-up interruption at Idaho National Lab	Unneeded electronics removed from emergency stop module
Too much power dissipated into Invert MOSFETS causing failure of inverter board and Power Factor Control	Redesigned charger electronics hardware for immunity to voltage interruptions and for automatic shutoff in abnormally low-efficiency conditions
High electromagnetic field radiated emissions	Data collected fro in-depth analysis. Research needed to determine best solution
EMF probe placed in gap between Tx and Rx resulting in 425 V/m, five times the public exposure limit	Measurement beyond scope of DOE requirements
EMF radiation exceeded SAE standard at ground to 20 cm and 40 cm positions	Further study and development needed
EMC capability electric field exceeded electric field limit	Further study and development needed

Table 9 - Problems and solutions

Alignment with SAE International Standards and Task Forces

In 2016, SAE International released J2954 TIR, the first step in standardization for wireless power transfer between infrastructure, vehicle suppliers and original equipment manufacturers (OEMs) for plug-in electric (PHEV) and electric vehicles (EVs). It covers frequency band, safety, interoperability, electromagnetic compatibility and electromagnetic field radiation limits as well as coil definitions.

The standard calls for a common charging frequency of 85 to 87 kilohertz (kHz) and three power classes for light-duty vehicle charging, up to 22 kW. The frequency band, safety, interoperability, EMC and EMF limits, and coil standard definitions enable any compatible vehicle to charge wirelessly from home, private and public chargers.

HATCI joined the SAE J2954 standards task force as a voting member and continuously monitored regulatory requirements. Most testing of its wireless power transfer project fell within SAE parameters:

- HATCI's frequency band targeted 80 to 100 kHz and was found to perform best around 88 kHz. However poor harmonics continued into the megahertz leading to excessive radiation.
- The 20 cm vertical coil gap between transmitter and receiver was within the SAE guideline
- SAE J2954's three charging classes bracket HATCI's testing and design – greater than 6.6 kW to 19.2 kW. The HATCI system was tested to 10 kW but higher charging power is possible.
- EMF radiation testing at HATCI found that electric and magnetic field levels inside the vehicles satisfied SAE requirements but were not satisfied from the ground to 40 cm and from the vehicle to 20 cm.
- Radiated emissions measured were below the proposed SAE limit of about 1.3 megahertz (MHz) except for a spike to 2 megahertz (MHz), which exceeded the limit. Conducted emissions did not meet the SAE requirement.

To assure interoperability with other SAE standards, HATCI team members joined the task forces for J2831 covering digital communication for wireless charging plug-in electric vehicles; J2836 developing use cases for wireless charging communication between plug-in electric vehicles and the utility grid; and J2847 overseeing wireless charging communication between plug-in electric vehicles and the utility grid.

Future Opportunities

Even with nascent growth in wireless charging, there are several areas of study and development that may change the trajectories of conductive (plug-in) and inductive (wireless) charging in future years. Advances in automatic alignment, dynamic charging while a vehicle is moving and extreme fast charging are among these opportunities.

Automatic Alignment

With a wireless power transmitter that evolved from a proof-of-concept to complete integration into a vehicle, the HATCI team is investigating functional improvement via an automatic alignment concept which would require little input from the driver to park on the charging pad.

Significant challenges including misalignment of the transmitter and receiver coils; cost, weight and packaging; electromagnetic field radiation; high temperatures and charging time, must be considered in the pursuit of sensorless alignment.

Dynamic Charging

Sensorless charging as being explored by HATCI could help advance dynamic charging, in which an electric vehicle is charged while in motion. An online electric vehicle course developed at the Korea Advanced Institute of Science and Technology is one example of a commercially available dynamic charging transportation system.

Numerous studies have reported that a benefit of dynamic charging is that it allows smaller and lighter batteries to be used due to frequent charging using the charging infrastructure embedded under roads.

In May 2017, Qualcomm demonstrated dynamic electric wireless charging (DVEC) on a test track at Satory Versailles, France. Two Renault vehicles were able to charge on the same track embedded with the charging tech at up to 20 kW while moving at high speed. [Qualcomm Demonstrates Dynamic Electric Vehicle Charging. (2017, May 18).

The four-year $10 million project was mostly funded by the European Commission with about 25 organizations and from nine European countries involved. [Electric cars could soon charge on the move. (2017, June 17).]

Testing is under way to evaluate the operation, safety and efficiency of energy transfer to the vehicles. A wide range of practical scenarios is being evaluated, including vehicle identification and authorization on entering the track, power level agreement between track and vehicle, and speed and alignment of vehicle along track. [Qualcomm Demonstrates Dynamic Electric Vehicle Charging. (2017, May 18).

Critics point to logistical hurdles in moving the technology to the highway. Among the objections are the massive cost of roadway tear-ups, the need to reserve one lane for vehicles capable of on-road charging, and the need to detect a non-chargeable car traveling on the road. Finally, there is the question of how electric cars charging dynamically would pay for the electricity they use.

Extreme Fast Charging

The economic impact of vehicle transportation on the national economy is staggering. More than 11 billion tons of freight worth $32 billion worth each day are moved by vehicles and carry people more than 3 trillion vehicle-miles. The opportunity to further reduce the amount of petroleum consumption, of which 70 percent of which goes to transportation, lies with greater production and adoption of electric vehicles. More EVs will require a charging infrastructure that can provide faster recharging than today, even with some Level 3 fast charging available. [Bowman, Z. DC fast charging for electric cars: what's here, what's coming, what's hype? (2017, May 23)

HATCI, like the DOE, sees the opportunity for wireless infrastructure, which enjoys a slight speed advantage over conductive charging but still requires 210-220 minutes to achieve a full state of charge, benefitting from Extreme Fast Charging (XFC). While HATCI's current WPC system is capable of charging at up to 19.2 kW, the future could see greater speeds, 150 kW or higher.

Developing these systems and batteries should allow plug-in electric vehicles to be charged much faster than current vehicle charging, enabling the greater use of electricity for transportation, 98 percent of which comes from a variety of domestic sources. By contrast, The U.S. sends more than $10 billion per month overseas for crude oil, and the average U.S. household spends nearly one-fifth of its total family expenditures on transportation, making it the number two spending category after housing. [EERE Funding Opportunity Announcements. (2017, October 10). Retrieved December 18, 2017]

Project Presentations

- 2013 DOE Vehicle Technologies Program Annual Merit Review and Peer Evaluation Meeting, May 13-17, 2013, Arlington, VA., Allan Lewis (HATCI) principal investigator
- Autotech Council Meeting; May 2013; Santa Clara, Calif., Afshin Partovi, Mojo Mobility
- Wireless Power Summit; December 2013; Austin, Texas, Afshin Partovi, Mojo Mobility
- 2014 DOE Vehicle Technologies Program Annual Merit Review and Peer Evaluation Meeting, June 16-20, 2014; Washington, D.C., Allan Lewis (HATCI), principal investigator; presenter John Robb
- Autotech Council Meeting; July 2014; Sunnyvale, Calif., Afshin Partovi, Mojo Mobility
- Wireless Power World; October 2014; Shanghai, China, Afshin Partovi, Mojo Mobility
- Sustain Summit; February 2015; Newport Beach, Calif., Afshin Partovi, Mojo Mobility
- KPMG's Automotive Executive Share Forum during NAIAS; January 2015; Detroit, Afshin Partovi, Mojo Mobility
- 2015 DOE Vehicle Technologies Program Annual Merit Review and Peer Evaluation Meeting, June 8-12, 2015; Arlington, VA, Allan Lewis (HATCI), principal investigator; presenter John Robb
- Wireless Power World Keynote Talk and Panel; September 2015; Beijing, China, Afshin Partovi, Mojo Mobility
- IDTechEx, November 18, 2015; Santa Clara, Calif., Afshin Partovi
- 2016 DOE Vehicle Technologies Program Annual Merit Review and Peer Evaluation Meeting, June 6-10, 2016; Washington, D.C., Rakan Chabaan, HATCI senior engineer
- Wireless Power Summit, October 5-6, 2017, Denver, Afshin Partovi, Mojo Mobility
- EVS30 Symposium, October 9-11, 2017, Stuttgart, Germany, Rakan Chabaan, HATCI senior engineer
- 3rd EVs & the Grid conference, October 17-19, 2017, San Francisco, Afshin Partovi, Mojo Mobility

Media Coverage

PR Newswire. Hyundai-Kia America Technical Center, Inc. And Mojo Mobility, Inc. Collaborate On Wireless Electric Vehicle Charging System

Based primarily on the press release above, the HATCI/Mojo wireless charging project received significant online media coverage between July 8 and 17, 2015, with some additional stories appearing later. Here is a sampling with internet links:

- USA Today. More automakers test wireless electric car charging
- Autoblog. Kia, Hyundai working on wireless charging with Mojo Mobility
- Green Car Congress. Hyundai-Kia America and Mojo Mobility partnering on wireless fast-charging project
- Fleets & Fuels. Mojo Eases Wireless Charging with HATCI
- Automotive News: http://www.autonews.com/article/20150710/OEM05/150719980/hyundai-kia-tech-firm-get-%246m-u.s.-grant-to-develop-wireless-ev
- Hybridcars.com http://www.hybridcars.com/hyundai-kia-developing-ev-wireless-charging/
- The Fast Lane Car, tflcar.com: http://www.tflcar.com/2015/07/hyundai-kia-working-wireless-charging-electric-vehicles-news/
- Carscoops.com: http://www.carscoops.com/2015/07/hyundai-and-kia-developing-wireless.html
- Motor Trend: http://www.motortrend.com/news/kia-tests-wireless-charging-system-using-soul-ev/

Project Summary

The objective of the project was to develop, implement, and demonstrate a wireless power transfer system (WPT) with total system efficiencies of more than 85 percent, power transfer at over 6.6 kW, charging at 80 to 100 kHz and maximum lateral positioning tolerance achievable while meeting emission guidelines.

Project Objectives

- Power transfer at greater than 6.6 kilowatts (kW)
- Total system efficiencies exceeding 85 percent
- Charging at 80 to 100 kilohertz (kHz)
- Vertical gap between ground transmitter (Tx) and receiver (Rx) of 20 cm

HATCI and its partner Mojo Mobility developed the wireless power transfer system with a minimum power transfer exceeding 6.6 kW. The wireless power transfer system was designed to operate via a 240V single phase input. In addition, HATCI tried to maximize wireless power transfer coil-to coil-lateral misalignment while meeting regulatory guidelines. The target misalignment tolerance was projected to be +/- 0.5 m along the width of the vehicle, later revised to +/-30cm; and +/-1m along the length of the vehicle, later revised to +/-40 cm. The 20 cm lateral coil-to-coil gap was evaluated for capability in real-world operation.

The work in Phase I originally included a cost analysis to show initial production costs for the system. In Phase II, the system was further developed and integrated into a Kia Soul EV. A commercial viability analysis of the system and cost benefits for components, both on-board and off-board the vehicle, was performed. In Phase III, real-world test results from a fleet of five Kia Soul models were demonstrated. All required safety and electromagnetic field (EMF) emission test results and real world performance results were obtained and provided to the DOE.

The overall project met or exceeded the objective to develop, implement, and demonstrate a wireless power transfer system (WPT) with total system efficiencies of more than 85 percent, power transfer at over 6.6 kW, average charging at 87 kHz and maximum lateral positioning tolerance achievable while meeting regulatory emission guidelines.

Dedicated Short Range Communications (DSRC) was dropped as the main communication and control protocol because of uncertainty about timeliness of wide auto industry adoption and challenges to allocations of frequencies along the 5.9 gigahertz (GHz) band. [(Federal Communications Commission; 2017, April 13)].

Instead, the communication system included real-time operating system (RTOS) software that resulted in fast response, more robustness and reduced susceptibility to communications disruptions and delays. A decision was made to run Wi-Fi, DC fast-charger CHAdeMO communications and a proportional integrated derivative controller (PID) in parallel.

Apart from iterative changes anticipated in developing the transmitter and receiver coils, problems encountered were relatively small and mostly manageable.

The application of higher voltage to the system during Phase II disrupted communications between the charger and the user control laptop. That was solved by using a Wi-Fi link between the charger and the laptop. Shielding was added to portion of transmitter board suspected of being subject to EMI disruptions.

Several issues were discovered during independent testing at Idaho National Laboratory beginning with an interruption to the initial power up of the system. This was quickly resolved by INL removing unnecessary electronics from its emergency stop module.

However, too much power being dissipated into invert MOSFETs caused the inverter board and Power Factor Control to fail, delaying INL testing for several months. The charger electronics hardware was redesigned for immunity to voltage interruptions and to automatically shut off the system in abnormally low-efficiency conditions.

The remaining issues involved EMF radiation levels exceeding INCIRP guidelines for human health. Some of the measurements taken at INL were outside the scope of DOE requirements for the project, but data was collected for in-depth analysis and further study.

The HATCI wireless power transfer system project was a success when measured against program objectives. Most problem areas during development were identified in advance. The table below outlines the performance objectives versus the actual results.

Performance Objectives	Actual Results
Power transfer at greater than 6.6 kW	System designed for power transfer up to 19.2 kW. Successfully tested to 10 kW
Total system efficiencies exceeding 85%	Peak total efficiency of 94% reached
Charging at 80 to 100 kHz	Consistently charged at 85 to 88 kHz
Vertical Z-gap between the ground transmitter (Tx) and receiver (Rx) of 20 cm	System consistently performed at 20 cm

Table 10: Performance objectives versus measured results

Appendix I – Glossary and Abbreviations

AC	Alternating Current
A/m	Amps per Meter
BEV	Battery Electric Vehicle – An electric vehicle that receives its power solely from batteries
BMS	Battery Management System
BOM	Bill of Materials
CAN	Controller Area Network – Robust vehicle standard that allows microcontrollers and devices to communicate with each other in applications without a host computer
CHAdeMO	Trade name of quick charging method for BEVs delivering up to 62.5 kW of direct current (500 volts, 125 amps) via a special electrical connector. Abbreviated from "CHArge de MOve," equivalent of "move using charge."
Conductive	Having the ability to transmit electricity through a physical path (conductor)
Connector	A conductive device that by insertion into a vehicle inlet establishes an electrical connection to the EV for the purpose of transferring energy and exchanging information.
DC	Direct Current
DSRC	Dedicated Short-Range Communications
DVEC	Dynamic Vehicle Electric Charging allows charging while in motion
ECU	Electronic Control Unit is an embedded unit that controls one or more of the electrical systems or subsystems in a vehicle
EMC	Electromagnetic Compatibility
EMF	Electromagnetic Field
EMI	Electromagnetic Interference – A disturbance generated by an external source that affects an electrical circuit by electromagnetic induction, electrostatic coupling or conduction
EV	Electric Vehicle, an automobile primarily powered by an electric motor that draws energy from a renewable energy storage device
EVSE	Electric Vehicle Supply Equipment – Equipment from the branch circuit to and including the connector that couples the EV inlet to transfer electric energy. Also a term for an EV charging station
FET	Field-Effect Transistor – A transistor that uses an electric field to control the electric behavior of a device
FOD	Foreign Object Detection

	Galvanic Isolation – A design technique that separates electrical circuits to eliminate stray currents.
GCEV	Grid Connected Electric Vehicle
GHz	Gigahertz
HATCI	Hyundai America Technical Center Inc.
INCIRP	International Commission on Non-Ionizing Radiation Protection
INL	Idaho National Laboratory
	Interoperability – Capability of a stands-conforming device to function as intended with other standards-conforming devices without special effort by the user
kHz	Kilohertz
kWh	Kilowatt Hour
	Level 1 Charging – A method that allows and EV to be connected to the most common grounded electrical receptacles (NEMA 5-15R and NEMA 5-20R). The vehicle shall be fitted with an on-board charger capable of accepting energy from the existing single phase alternating current (AC) supply network.
	Level 2 Charging - A method that uses dedicated AC EV supply equipment in either private or public locations. The vehicle shall be fitted with an on-board charger capable of accepting energy from single phase alternating current (AC) electric vehicle supply equipment.
	Litz wire – A type of cable used in electronics to carry alternating current. The wire is designed to reduce the skin effect and proximity effect losses in conductors used at frequencies up to about 1 megahertz (MHz).
	Magnetic Gap – The distance between two wireless power transfer (WPT) coils
MR	Magnetic Resonant
MOSFET	Metal-Oxide Semiconductor Field-Effect Transistor
Mojo	Mojo Mobility
NFP	Near Field Power
NREL	National Renewable Energy Lab
OEM	Original Equipment Manufacturer
	Off-board Charger – A charger located off-board the vehicle.
	On-board Charger – A charger located on the vehicle.

PCB	Printed Circuit Board -- A method to connect electronic components using conductive tracks, pads and other features etched from copper sheets laminated onto a non-conductive substrate.
PFC	Power Factor Correction -- A feature included in some computer and other power supply boxes that reduces the amount of reactive power generated by a computer.
PID	Proportional Integrated Derivative Controller
	Power Receiver – The subsystem of the WEVSE (vehicle side) that acquires near field inductive power and controls its availability at its output. For this purpose, the Power Receiver communicates its power requirements to the Power Transmitter.
	Power Transmitter – The subsystem of the WEVSE (primary) that generates near field inductive power and controls its transfer to a Power Receiver.
	Primary Coil – A component of a Power Transmitter that converts electric current into magnetic flux
	Proximity Circuit – A circuit that defines the state of the charge connector in reference to the vehicle inlet. For AC charging, the PEV and coupler contain a proximity circuit that the PEV uses to detect connection of the EVSE connector to the PEV inlet. The proximity circuit is modified for DC charging so that the EVSE can also sense that the cord is plugged into the PEV inlet.
PWM	Pulse Width Modulation -- A modulation technique that rapidly turns the switch between supply and load on and off. The proportion of “on” time to total time is called the duty cycle.
RFID	Radio Frequency Identification
RTOS	Real-time Operating System
Rx	Wireless Receiver
SAE	SAE International
	Secondary Coil – The component of a Power Receiver that converts magnetic flux to electromotive force
SCR	Silicon Controlled Rectifier – A four-layer solid-state current-controlling device that uses a p-n-p-n semiconductor structure.
SoC	State of Charge
THD	Total Harmonic Distortion
Tx	Wireless Transmitter
V	Volts
V/m	Volts per Meter
WEVSE	Wireless Electric Vehicle Supply Equipment

Wi-Fi 802.11n -- A wireless (Wi-Fi) standard introduced in 2007. It supports MIMO (multiple in, multiple out) data transfers, which can transmit multiple streams of data at once.

WPT Wireless Power Transfer -- The transfer of electrical power from the AC supply network to the electric vehicle by contactless means.

x-axis Fore to aft measurement along a vehicle

y-axis Side-to-side measurement in front of a vehicle

z-gap Vertical distance between the transmitter and receiver in a wireless power transfer system

Appendix 2 – Table of Figures and Charts

Figures

Tables

Appendix 3 - References

Communication between Wireless Charged Vehicles and Wireless EV Chargers. (2015, August 5). Retrieved November 19, 2017, from http://standards.sae.org/wip/j2847/6/

Dedicated Short Range Communications (DSRC) Service. (2017, April 13). Retrieved November 19, 2017, from https://www.fcc.gov/wireless/bureau-divisions/mobility-division/dedicated-short-range-communications-dsrc-service

Development of Design and Engineering Recommendations for In-Vehicle Alphanumeric Messages. (2012, April 26). Retrieved November 19, 2017, from http://standards.sae.org/j2831_201204/

EERE Funding Opportunity Announcements. (2017, October 10). Retrieved December 18, 2017, from https://eere-exchange.energy.gov/Default.aspx?Search=DE-FOA-0001808&SearchType=

Electric cars could soon charge on the move. (2017, June 17). Retrieved November 14, 2017, from https://economictimes.indiatimes.com/industry/auto/news/passenger-vehicle/cars/electric-cars-could-soon-charge-on-the-move/articleshow/59118553.cms

Guidelines for Limiting Exposure to Time-Varying Electric and Magnetic Fields (1Hz to 100 KHz): Erratum. (2011). *Health Physics,100*(1), 112. doi:10.1097/01.hp.0000391657.33635.13

Ingram, A. (2014, April 14). Toyota Gasoline Engine Achieves Thermal Efficiency Of 38 Percent. Retrieved November 19, 2017, from https://www.greencarreports.com/news/1091436_toyota-gasoline-engine-achieves-thermal-efficiency-of-38-percent

Jerram, L., Gartner, J., & Abuelsamid, S. (2015). *Wireless Charging Commercial Viability Analysis* (pp. 5-14, Publication). Navigant Research.

Kettles, D. (2015). Electric Vehicle Charging Technology Analysis and Standards. Cocoa. Retrieved from http://fsec.ucf.edu/en/publications/pdf/FSEC-CR-1996-15.pdf

Neubauer, J., Wood, E., Burton, E., Smith, K., & Pesaran, A. (2015, May 3). Impact of Fast Charging on Life of EV Batteries. Retrieved November 14, 2017, from https://www.nrel.gov/docs/fy15osti/63700.pdf

Presented at EVS28, KINTEX, Korea, May 3-6, 2015

Qualcomm Demonstrates Dynamic Electric Vehicle Charging. (2017, May 18). Retrieved November 14, 2017, from https://www.qualcomm.com/news/releases/2017/05/18/qualcomm-demonstrates-dynamic-electric-vehicle-charging

SAE International Approves TIR J2954 for PH/EV Wireless Charging. (2016, May 17). Retrieved November 19, 2017, from https://www.sae.org/news/3391/

SAE J2954 Wireless Power Transfer and Alignment Task Force. (n.d.). Retrieved November 19, 2017, from https://www.sae.org/works/committeeHome.do?comtID=TEVHYB10